

~~38/75-78~~
Special Disty

WAPD-TM-1377
DOE RESEARCH AND
DEVELOPMENT REPORT

**METHODS FOR ASSESSING
HOMOGENEITY IN ThO₂-UO₂ FUELS
(LWBR Development Program)**

JUNE 1978

MASTER

CONTRACT EY-76-C-11-0014

DISTRIBUTION OF THIS DOCUMENT IS UNLIMITED

**BETTIS ATOMIC POWER LABORATORY
WEST MIFFLIN, PENNSYLVANIA**

**Operated for the U. S. Department of Energy by
WESTINGHOUSE ELECTRIC CORPORATION**



DISCLAIMER

This report was prepared as an account of work sponsored by an agency of the United States Government. Neither the United States Government nor any agency Thereof, nor any of their employees, makes any warranty, express or implied, or assumes any legal liability or responsibility for the accuracy, completeness, or usefulness of any information, apparatus, product, or process disclosed, or represents that its use would not infringe privately owned rights. Reference herein to any specific commercial product, process, or service by trade name, trademark, manufacturer, or otherwise does not necessarily constitute or imply its endorsement, recommendation, or favoring by the United States Government or any agency thereof. The views and opinions of authors expressed herein do not necessarily state or reflect those of the United States Government or any agency thereof.

DISCLAIMER

Portions of this document may be illegible in electronic image products. Images are produced from the best available original document.

Special External Distribution

METHODS FOR ASSESSING HOMOGENEITY
IN ThO₂-UO₂ FUELS
(LWBR Development Program)

R. M. Berman

June 1978

Contract EY-76-C-11-0014

Printed in the United States of America
Available from the
National Technical Information Service
U. S. Department of Commerce
5285 Port Royal Road
Springfield, Virginia 22151

MASTER

6000
8000

NOTICE
This report was prepared as an account of work sponsored by the United States Government. Neither the United States nor the United States Department of Energy, nor any of their employees, nor any of their contractors, subcontractors, or their employees, makes any warranty, express or implied, or assumes any legal liability or responsibility for the accuracy, completeness or usefulness of any information, apparatus, product or process disclosed, or represents that its use would not infringe privately owned rights.

NOTE

This document is an interim memorandum prepared primarily for internal reference and does not represent a final expression of the opinion of Westinghouse. When this memorandum is distributed externally, it is with the express understanding that Westinghouse makes no representation as to completeness, accuracy, or usability of information contained therein.

6000
8000

BETTIS ATOMIC POWER LABORATORY
WEST MIFFLIN, PENNSYLVANIA

Operated for the U. S. Department of Energy by
WESTINGHOUSE ELECTRIC CORPORATION

DISTRIBUTION OF THIS DOCUMENT IS UNLIMITED

— NOTICE —

This report was prepared as an account of work sponsored by the United States Government. Neither the United States nor the United States Department of Energy, nor any of their employees, nor any of their contractors, subcontractors, or their employees, make any warranty, express or implied, or assumes any legal liability or responsibility for the accuracy, completeness or usefulness of any information, apparatus, product or process disclosed, or represents that its use would not infringe privately owned rights.

FOREWORD

The Shippingport Atomic Power Station located in Shippingport, Pennsylvania was the first large-scale, central-station nuclear power plant in the United States and the first plant of such size in the world operated solely to produce electric power. This project was started in 1953 to confirm the practical application of nuclear power for large-scale electric power generation. It has provided much of the technology being used for design and operation of the commercial, central-station nuclear power plants now in use.

Subsequent to development and successful operation of the Pressurized Water Reactor in the DOE-owned reactor plant at the Shippingport Atomic Power Station, the Atomic Energy Commission in 1965 undertook a research and development program to design and build a Light Water Breeder Reactor core for operation in the Shippingport Station. In 1976, with fabrication of the Light Water Breeder Reactor (LWBR) nearing completion the Energy Research and Development Administration established the Advanced Water Breeder Applications program (AWBA) to develop and disseminate technical information which would assist U.S. industry in evaluating the LWBR-concept. All three of these reactor development projects have been administered by the Division of Naval Reactors with the goal of developing practical improvements in the utilization of nuclear fuel resources for generation of electrical energy using water-cooled nuclear reactors.

The objective of the Light Water Breeder Reactor project has been to develop a technology that would significantly improve the utilization of the nation's nuclear fuel resources employing the well-established water reactor technology. To achieve this objective, work has been directed toward analysis, design, component tests, and fabrication of a water-cooled, thorium oxide fuel cycle breeder reactor to install and operate at the Shippingport Station. Operation of the LWBR core in the Shippingport Station started in the Fall of 1977 and is expected to be completed in about 3 to 4 years. Then the fissionable fuel inventory of the core will be measured. This effort, when completed in about 2 to 3 years after completion of LWBR core operation, is expected to confirm that breeding actually took place.

The Advanced Water Breeder Applications (AWBA) project was initiated to develop and disseminate technical information that will assist U.S. industry in evaluating the LWBR concept for commercial-scale applications. The project will explore some of the problems that would be faced by industry in adapting technology confirmed in the LWBR program. Information to be developed includes concepts for commercial-scale prebreeder cores which will produce uranium-233 for light water breeder cores while producing electric power, improvements for breeder cores based on the technology developed to fabricate and operate the Shippingport LWBR core, and other information and technology to aid in evaluating commercial-scale application of the LWBR concept.

Technical information developed under the Shippingport, LWBR, and AWBA projects has been and will continue to be published in technical memoranda, one of which is this present report.

CONTENTS

	<u>Page</u>
I. INTRODUCTION: THE NATURE OF INHOMOGENEITIES	1
II. LWBR BINARY SPECIFICATIONS	5
III. ELECTRON PROBE TRAVERSSES	6
A. Applications	6
B. Sample Preparation	6
C. Interpretation of Results	7
D. Typical Results	10
IV. AUTORADIOGRAPHY	13
A. Sample Preparation	13
B. Calibration	13
C. Correction for α -Particle Range	14
D. Use of Microdensitometer	16
E. Interpretation of Microdensitometer Profiles	18
F. Criteria for Rejecting Artifacts	18
V. SUMMARY AND CONCLUSION	21
ACKNOWLEDGMENTS	24
REFERENCES	24
APPENDIX I. AVERAGE TRAVERSE INCREMENT CAUSED BY INCREASE IN APPARENT DIAMETER OF INHOMOGENEITIES BY ALPHA-PARTICLE RANGE	25
APPENDIX II. LWBR CORE REFERENCE PROCEDURE	29

LIST OF TABLES

<u>Table</u>	<u>Title</u>	<u>Page</u>
I	Specification of the Maximum Volume Percent of Inhomogeneities Permitted in LWBR Binary Fuel (Reference 3)	5

LIST OF FIGURES

<u>Figure</u>	<u>Title</u>	<u>Page</u>
1	Typical Electron Probe Scans Across a Sample of Binary Material	11
2	Electron Probe Profiles Across a Typical Interface	12
3	Typical Microdensitometer Traverses, Showing Method of Profile Correction	17

LIST OF FIGURES (Cont)

<u>Figure</u>	<u>Title</u>	<u>Page</u>
4	Autoradiograph of Sample A (10x)	20
5	Autoradiograph of Sample R (10x)	21
6	Microdensitometer Traverses Across the Edges of Sample A (Good Contact) and Sample R (Poor Contact)	22

$\text{ThO}_2\text{-UO}_2$ solid solutions fabricated as LWBR fuel pellets are examined for uniform uranium distribution by means of autoradiography. Kodak NTA plates are used. Images of inhomogeneities are 29 ± 10 microns larger in diameter than the high-urania segregations that caused them, due to the range of alpha particles in the emulsion, and an appropriate correction must be made. Photographic density is approximately linear with urania content in the region between underexposure and overexposure, but the slope of the calibration curve varies with aging and growth of alpha activity from the parasitic U^{232} and its decomposition products. A calibration must therefore be performed using two known points--the average photographic density (corresponding to the average composition) and an extrapolated background (corresponding to zero urania).

As part of production pellet inspection, plates are evaluated by inspectors, who count segregations by size classes. This is supplemented by microdensitometer scans of the autoradiograph and by electron probe studies of the original sample if apparent homogeneity is marginal.

METHODS FOR ASSESSING HOMOGENEITY IN $\text{ThO}_2\text{-UO}_2$ FUELS

R. M. Berman

I. INTRODUCTION: THE NATURE OF INHOMOGENEITIES

The prevention of local fissile material overload, or rather its restriction within acceptable bounds, is among the problems confronting the fuel element designer and fuel fabricator. Local regions of a fuel pellet having too high a loading of fissile material will operate at a higher temperature than the design calls for. They will deplete at a greater rate, and produce a larger volume of fission products. This effect is in addition to the effects of higher temperature, which will increase local fuel swelling and cause a larger proportion of the total fission gases to be released.

This report describes the measures adopted by the Bettis Atomic Power Laboratory during the manufacture of the Light Water Breeder Reactor (LWBR) to ensure that fuel inhomogeneity was consistent with fuel pellet design limits

for this attribute. The LWBR program is under the technical direction of the Division of Naval Reactors of the Department of Energy, and the first reactor core of this type has been installed in the Department's pressurized-water thermal reactor plant at Shippingport, Pa. The operation of this LWBR core is expected to confirm that the breeding of fissile material can be achieved in a pressurized, light-water, thermal-neutron plant using a thoria and thoria-urania binary fuel system. This core represents the first large-scale fabrication of thoria-base fuels of high density, and the first use of uranium-233 in ceramic fuel for a power reactor.

The LWBR core is a seed-blanket configuration with an inner region containing 12 movable seed assemblies. These assemblies contain thoria-urania fuel of compositions varying from about 1 to 6 wt% urania in thoria. The compositions are arranged in zones, and control is accomplished by moving zones of greater or less urania content into the central region of the core. There are no neutron-absorbing control rods. This report deals with the methods taken to inspect these fuels for homogeneity.

These binary fuels are solid solutions; given enough time, sufficiently elevated temperatures, and sufficiently small segregations high in urania or thoria, they would tend to homogenize by diffusion. Absolutely uniform uranium distribution would require infinite time, but it is possible to calculate a finite annealing or sintering time that would be sufficient to bring the entire range of composition within any specified limits. Reference 1 discusses this calculation; its conclusions are reviewed below.

The interdiffusion coefficient D of urania and thoria is given by the equation:

$$D = 1.125 \times 10^{-5} \exp(-62200/RT) \text{ cm}^2/\text{sec} \quad (\text{Eq. 1})$$

For a sintering temperature $T = 1750\text{C} = 2023\text{K}$, $D = 2.142 \times 10^{-12} \text{ cm}^2/\text{sec}$. The sintering time, t , is equal to 12 hours or $4.32 \times 10^4 \text{ sec}$. For a typical sintering run, therefore, $Dt = 9.254 \times 10^{-8} \text{ cm}^2$.

Rhines and Colton (Reference 2) proposed an index of homogeneity, h , such that:

$$h = a^2/(Dt) \quad (\text{Eq. 2})$$

where a is the grain diameter, or more precisely, the distance between the center of a urania segregation or particle and the center of an adjacent thoria

segregation or particle. In a perfectly homogeneous sample, $h = 0$. Reference 1 proposed a value of $h = 10$ as representing a satisfactorily uniform uranium distribution for ceramic nuclear fuel. This would imply that the centers of the surviving inhomogeneities would have a urania content approximately 50% higher than the mean composition. Evaluation of Equation 2 for $h = 10$ gives a value of $a = 9.69$ micrometers (μm).

As the value of a increases above $10\mu\text{m}$, the value of h increases as its square, and it soon reaches a value ($h > 100$) at which the fuel at the center of the inhomogeneity is essentially pure urania. In this case, the thoria-urania interface consists of a band of intermediate compositions at the surface of a sphere with a radius considerably larger than the width of the band. Therefore, the curvature of the band region may be ignored. The interface may be regarded as an infinite plane, and the radial composition profile developed across this interface is such that:

$$M(x,t) = 0.5 + 0.5 \operatorname{erf} [x/(2\sqrt{Dt})] \quad (\text{Eq. 3})$$

where $M(x,t)$ is the mole fraction of urania at distance x from the interface, at time t , and "erf" represents the error function. $M(x,t)$ never reaches 1; however, for $[x/(2\sqrt{Dt})] = 1$, $M(x,t) = 0.9213$, which may reasonably be regarded as the outer margin of the region of nearly pure urania. For $Dt = 9.254 \times 10^{-8} \text{ cm}^2$, the corresponding value of x is $6.084\mu\text{m}$ from the original interface. If, at the time a pellet of binary fuel is introduced into the sintering furnace, it contains fragments of urania with radii larger than this value, each of the fragments will develop a diffusion band extending this distance on both sides of the initial position of the interface. The resulting diffusion band, after a sintering run of 12 hours at 1750°C , will be approximately $12\mu\text{m}$ wide, and will vary in composition from $\text{ThO}_2\text{-}8 \text{ mol\% UO}_2$ on its outer edge, to $\text{ThO}_2\text{-}92 \text{ mol\% UO}_2$ on its inner edge.

If the inhomogeneity consisted initially of a large particle of pure urania, the fuel remaining inside the inner margin of the diffusion zone, a region with a diameter approximately $12\mu\text{m}$ smaller than the initial grain before sintering, will consist of almost pure UO_2 . However, it may contain considerable porosity. Uranium diffuses through the interface at a higher rate than thorium (References 3 and 4). As a result, void space appears and accumulates on the urania-rich margin of the diffusion zone. This is known as the Kirkendall Effect.

It acts in a favorable way, and tends to nullify the deleterious effects of the inhomogeneity; it reduces the loading, and provides additional porosity for the additional fission gas, at precisely the locality where it is needed. On the other hand, the large, elongated pores formed by the Kirkendall Effect tend to decrease the thermal conductivity, and therefore increase the temperature, also at precisely the point where this is undesirable.

Most inhomogeneities in LWBR binary fuel pellets probably originated as single large urania particles, as described above. They range from spherical to sub-angular in shape, with rounded corners and approximately equiaxial dimensions, at least up to a mean diameter of 250 μm . Typical diameters are 150 μm or less. Elliptical bodies are also occasionally observed. Inhomogeneities of this type consist of a diffusion zone, 12 μm wide, within which lies a region of nearly pure urania with a varying amount of Kirkendall-generated porosity. The local density is between 70 and 98% of the theoretical maximum; larger inhomogeneities have less Kirkendall-generated porosity.

However, another type of inhomogeneity was also observed in production samples of LWBR binary fuel pellets. These consisted of regions with dimensions as large as 500 μm . The composition within these atypical regions was uniform and very much lower in urania than the type of inhomogeneity described previously. Typical urania content was 5 to 10 mol%. The amount and distribution of porosity in these regions are much like that in the remainder of the material. The grain size is somewhat larger, and is comparable to the size that would be expected in a similarly sintered uniform pellet with the somewhat elevated urania content of the inhomogeneity. (Grain size is a function of composition in high-thoria binary material, and increases with increasing urania content.) Electron probe scans show that a diffusion zone exists at the margin, but it is not a particularly prominent feature of these large, dilute inhomogeneities. It is postulated that these segregations arose during the micronizing and agglomerating processes. During micronizing, the stream of air that carries the particles in the mill may segregate the urania grains, perhaps due to their greater density. As a result, slight concentrations may be formed, and escape the homogenization process by lodging in the micronizer dust collection bags.

The fuel powder after micronizing is passed to the agglomeration stage, in which the fuel is mixed with Carbowax and granulated on a 25-mesh screen. This screen has openings 711 μm square; and no atypical inhomogeneities larger than

this have been observed. Instead, they are just smaller, and they may have been shaped by being forced through the sieve holes. Their observed shape may be a random cross-section of such a sieve-extruded body.

II. LWBR BINARY SPECIFICATIONS

Specifications for the maximum amount of inhomogeneity volume permitted in LWBR binary fuel are set forth in Table I. They are calculated on the assumption that the inhomogeneities consist of 100% dense, pure urania. The values of Table I are those at which, for a probability level $P = 0.95$, no more than 5% of the uranium content of a fuel rod, or 10% of the uranium content of a pellet, is located in the inhomogeneities. There is a further requirement that no individual inhomogeneities with a mean diameter greater than $381\mu\text{m}$ be observed, except as corrected in the following section.

TABLE I. SPECIFICATION OF THE MAXIMUM VOLUME PERCENT OF INHOMOGENEITIES PERMITTED IN LWBR BINARY FUEL (REFERENCE 3)

Region	Approximate Region Loading w/o UF	Limit (Volume Percent)	
		Blend Median	Individual Pellet
Seed			
Hi Zone	5.195	0.29 v/o	0.58 v/o
Lo Zone	4.327	0.29 v/o	0.44 v/o
Std. Blanket			
Hi Zone	2.000	0.105 v/o	0.215 v/o
Med Zone	1.662	0.09 v/o	0.18 v/o
Lo Zone	1.211	0.09 v/o	0.125 v/o
P.F. Blanket			
Hi Zone	2.733	0.145 v/o	0.295 v/o
Med Zone	2.005	0.105 v/o	0.215 v/o
Lo Zone	1.649	0.105 v/o	0.18 v/o

In this evaluation, the mean diameters of large, dilute polygonal inhomogeneities are revised downward from their actual observed value to an "equivalent diameter". The ratio between the equivalent diameter, d_e , and the observed diameter, d_o , is calculated as follows:

$$\frac{d_e}{d_o} = \sqrt{\frac{100 - U_B}{U_O - U_B}} \quad (\text{Eq. 4})$$

where d_o is the mean diameter, and U_0 the mean composition in w/o UO_2 , of the inhomogeneity; U_B is the w/o UO_2 in the bulk composition; and d_e is the equivalent diameter. The dilute inhomogeneity is treated in the evaluation as if it were a fully dense, 100 w/o UO_2 inhomogeneity of the equivalent diameter.

The values given in Table I are expressed in terms of vol% inhomogeneity (v/o). In fact, inhomogeneities are observed as areas on a random plane through a pellet, or, in the case of electron probe traverses, as segments of a random line on such a surface. However, the surface is the summation of all possible lines parallel to the given traverse, and the volume is the summation of an infinite number of planes parallel to the one exposed. If the surface, or traverse, is indeed typical, then the area fraction of inhomogeneity exposed in the surface, and the linear fraction exposed in a traverse, corresponds to the volume fraction in the sample. The volume varies as the cube of the diameter, but a segment of a random traverse is not the diameter (in the general case). The assumption of a linear relationship (rather than one varying as the cube) between the traverse and the volume precisely compensates for this. The relationship between areas measured in a random surface and volume fractions in the sample is analogous, and the relationship is once again linear.

III. ELECTRON PROBE TRAVERSES

A. Applications

The principal methods for evaluating the extent of inhomogeneity in binary fuels are by means of the electron probe and autoradiography. Autoradiography is a production tool; it is relatively inexpensive and can be carried out in a routine manner. The electron probe is a research tool, which is very much slower and more expensive to use. Lengthy sample preparation is required, as well as virtually constant attention during the scanning of the sample. The electron probe is available to calibrate and to check the results obtained by autoradiography, particularly if a marginal situation arises. Also, reference to electron probe results can be utilized whenever there is a substantial change in the standard evaluation procedures based on autoradiography.

B. Sample Preparation

Samples for the electron probe are mounted, ground, and polished using standard metallographic techniques. It is then necessary to coat the sample with a layer of carbon about 300A thick, in order to render it electrically

conductive. This is done by placing the sample in a vacuum chamber, and striking an arc between two standard carbon spectrographic electrodes, approximately 20 cm removed from the surface to be coated. The arc is continued for approximately five minutes.

Uranium content is determined from the intensity of the first-order uranium $M\beta$ x-ray emission, at a wavelength of 3.7155 \AA . A focussed beam of optimum sharpness (3 μm diameter) should be used; its intensity should be adjusted to give a satisfactory chart recording without damaging the specimen, and to permit reasonable scanning times.

C. Interpretation of Results

Ogilvie (Reference 5) gives a series of empirical equations for relating the observed peak intensity to the composition in binaries such as thoria-urania solid solutions. Although in fact the equations are based on observations on much lighter elements, they may be taken as reasonable approximations. In the following presentation, the variables are defined in terms of their specific application to the uranium $M\beta$ peak in thoria-urania solid solutions.

It is possible to define a single conversion parameter, a_{AB} , such that

$$\frac{1 - K_A}{K_A} = a_{AB} \frac{1 - C_A}{C_A} \quad (\text{Eq. 5})$$

where

K_A = intensity of the uranium $M\beta$ peak, as a fraction of that expected from a sample of pure uranium

C_A = the mole fraction of uranium.

Ogilvie then gives the following expression for a_{AB} ,

$$a_{AB} = 0.95 \left[\frac{\sigma + X_B^A}{\sigma + X_A^A} \right] \left[\frac{Z_A}{Z_B} \right]^{0.3} \left[\frac{1}{1 + 0.07 k} \right] \quad (\text{Eq. 6})$$

where

σ = absorption cross-section of 30 KV electrons = 1820 gm cm^{-4}

Z_A = atomic number of uranium = 92

Z_B = atomic number of thorium = 90

X_B^A = mass absorption coefficient for Uranium $M\beta$ radiation in thorium
= 578.3 gm cm^{-1}

X_A^A = mass absorption coefficient of U M β radiation in uranium = 618.9 gm cm⁻⁴

k = a quantity that is significant only for wavelengths near the K absorption edges of one of the elements present. In this case, k \approx 0.

Evaluation of Equation 6 gives $a_{AB} = 0.9404$. However, the initial coefficient (0.95) is somewhat uncertain; it may be nearly unity for heavy elements such as uranium and thorium. The coefficient a_{AB} may therefore be taken as unity, and Equation 5 reduces to a linear relationship between peak intensity and molar composition. For calibration purposes, therefore, it is sufficient to establish two points: the background, which represents zero uranium, and the average intensity, which represents the bulk composition.

Background is measured by making an angular scan in the vicinity of the uranium M β peak, and observing the intensity at some distance from the peak. In the traverses of the specimen, lower values than this may be observed; these are indications that the electron beam has encountered a pore. This may be confirmed by observing that the thorium signal also disappears at this point.

Straight traverses are run, covering approximately three to four millimeters of linear distance on the sample. Generally speaking, the starting point and direction should be chosen at random, unless it is desired to explore some special feature on the sample surface. (The sample, and the spot actually being measured, can be determined and observed through an optical microscope that is integral with the electron probe.)

Both thorium and uranium scans have been run. However, it has been the general experience that the thorium scans add no additional information, and are less sensitive to the changes usually observed at inhomogeneities. Therefore it has been the practice at Bettis to expend any additional experimental effort on additional uranium scans, rather than on thorium scans that merely corroborate previous observations.

Average intensities may be determined by reading the recorder chart at a definite interval, such as 50 microns. Readings corresponding to voids (i.e., below normal background) are omitted from the computation of the average. Then the composition C, in w/o UO₂, is calculated for any recorder chart reading R as follows:

$$\frac{C}{C_A} = \frac{R - B}{R_A - B} \quad (\text{Eq. 7})$$

where

- C = composition of point being observed, in w/o UO_2
- C_A = bulk composition, w/o UO_2
- R, R_A = recorder chart readings corresponding to C and C_A
- B = background.

The composition gradients shown on the recorder chart are slightly less steep than those on the actual sample. This is due to the fact that the beam focus has a finite diameter, 3 microns, at the recommended settings. If such a beam should cross an infinitely sharp interface between low- and high-urania regions, the recorder trace would begin to rise as soon as the leading edge crossed the interface, and would not complete its rise until the trailing edge crossed it. The departure of the resulting S-shaped curve from a straight vertical line represents, in general magnitude, the change in slope of all the observed gradients.

Detailed methods for correcting the profiles for this effect are discussed in Reference 1. They are unnecessary, however, for the study of inhomogeneities in sintered binaries. The extent of diffusion on sintering controls the scale of the smallest significant features of the composition profile; features surviving the sintering process must have a minimum diameter of ten microns, three times the beam diameter. For features this size, the average and maximum urania content correspond closely to the values calculated by means of Equation 7 from the recorder chart.

A measure of the size of the feature may be obtained by determining the distance between the mid-points of the diffusion profiles of the margins, as indicated on the recorder chart.

The resulting recorder traces may be evaluated by making use of the fact that the amount of uranium present is proportional to the area under the curve and above background. It is therefore necessary to compare the area of the peaks representing the inhomogeneities with the total area above background; if the peaks are less than five percent of the total, the sample meets the specifications.

Since the volume fraction of inhomogeneity is proportional to the linear fraction along a random traverse, and the amount of uranium present is proportional to the peak height, the amount of uranium in an inhomogeneity is proportional to its area on the recorder chart. It is therefore not necessary to

treat each inhomogeneity individually, for example, by squaring its diameter, as is the case with autoradiographic study of the entire surface. Instead, it is possible to deal with a total area of the inhomogeneity peaks. This is an important advantage of the electron probe method.

An inhomogeneity, in sintered LWBR binary fuel pellets, may be defined as a segment of the traverse more than 10 microns long, with a composition continuously in excess of 3 w/o UO_2 above nominal, except for voids. Minor fluctuations over the 3 w/o-above-nominal threshold should be ignored. The total volume of inhomogeneity, so defined, corresponds closely to the value determined by routine autoradiographic inspection. That is, these limits correspond closely to the threshold at which a human evaluator makes the subjective, qualitative decision that an inhomogeneity is present.

After the inhomogeneities are identified on the recorder trace, their areas on the chart paper should be measured. For each, this will be a region bounded by the recorder trace, the background level, and two connecting vertical lines at the point at which the recorder trace crosses the 3 w/o-over-nominal threshold. This area may be found by planimeter, by counting the squares of the imprinted grid on the recorder paper, or by making a xerographic copy, cutting out the images, and weighing them.

Since the average amplitude of the recorder trace has already been found in the process of calibration, the total area above background can be found by multiplying this average amplitude by the length of the recorder chart. Then the fraction of total uranium in the inhomogeneities can be found by dividing the area of the peaks by the total area above background.

D. Typical Results

Electron probe scans of binary materials are shown in Figures 1 and 2. The peaks of Figure 1 are typical of large, nearly pure UO_2 particles surviving the manufacturing process; the sample consisted of ThO_2 - 2.28 w/o $U^{235}O_2$ from a pre-production run. Figure 2 shows the margin of a large, dilute polygonal inhomogeneity. The calculated curve in Figure 2 shows the slopes of the profile to be expected from diffusion across a sharp interface during the sintering run. The actual measured profile appears slightly less steep, due to the finite size of the electron beam. The displacement of the calculated profile to the left of the measured profile has no physical significance; it was done for purposes

MOUNT #4903J

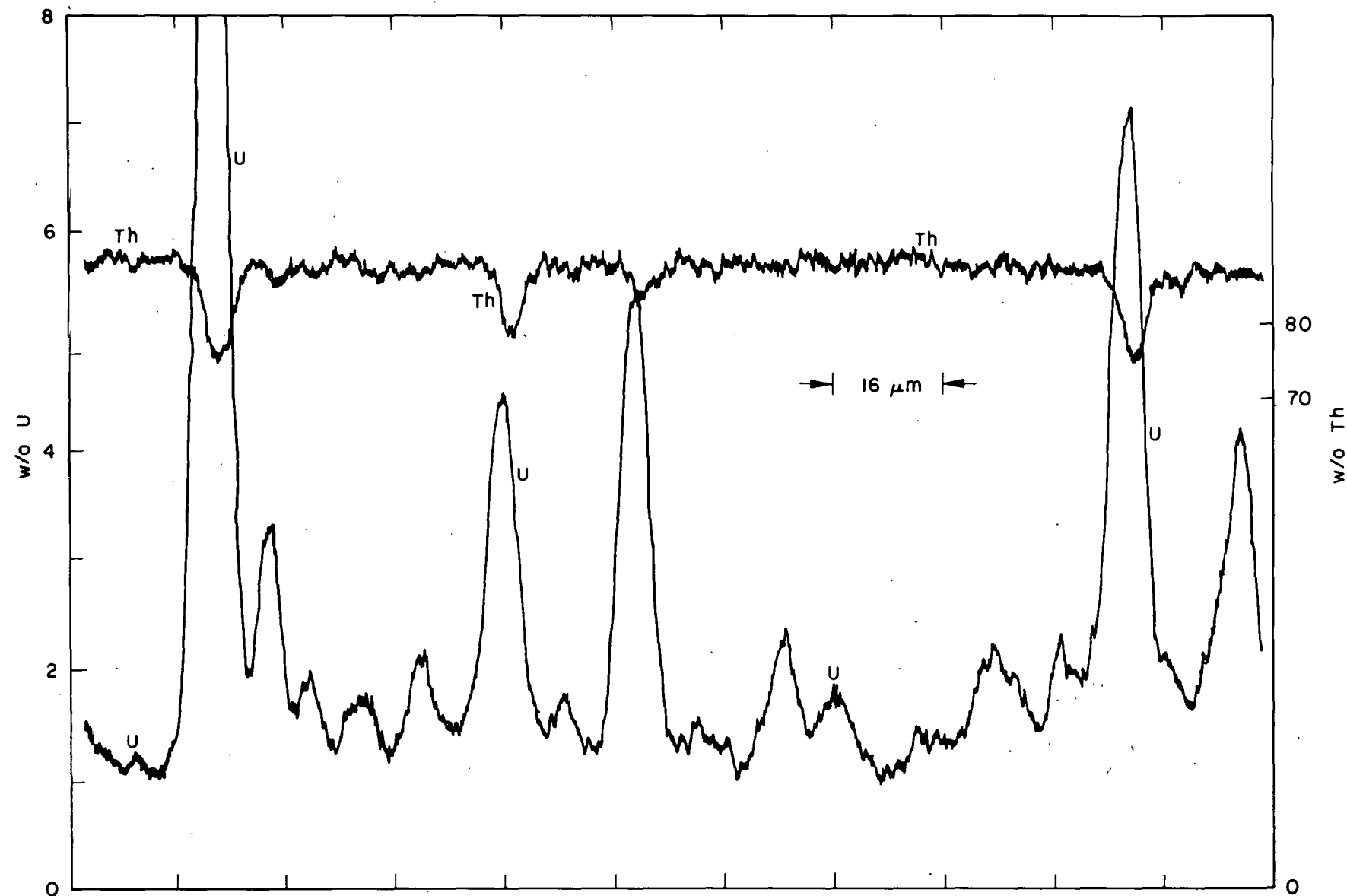


Figure 1. Typical Electron Probe Scans Across a Sample of Binary Material

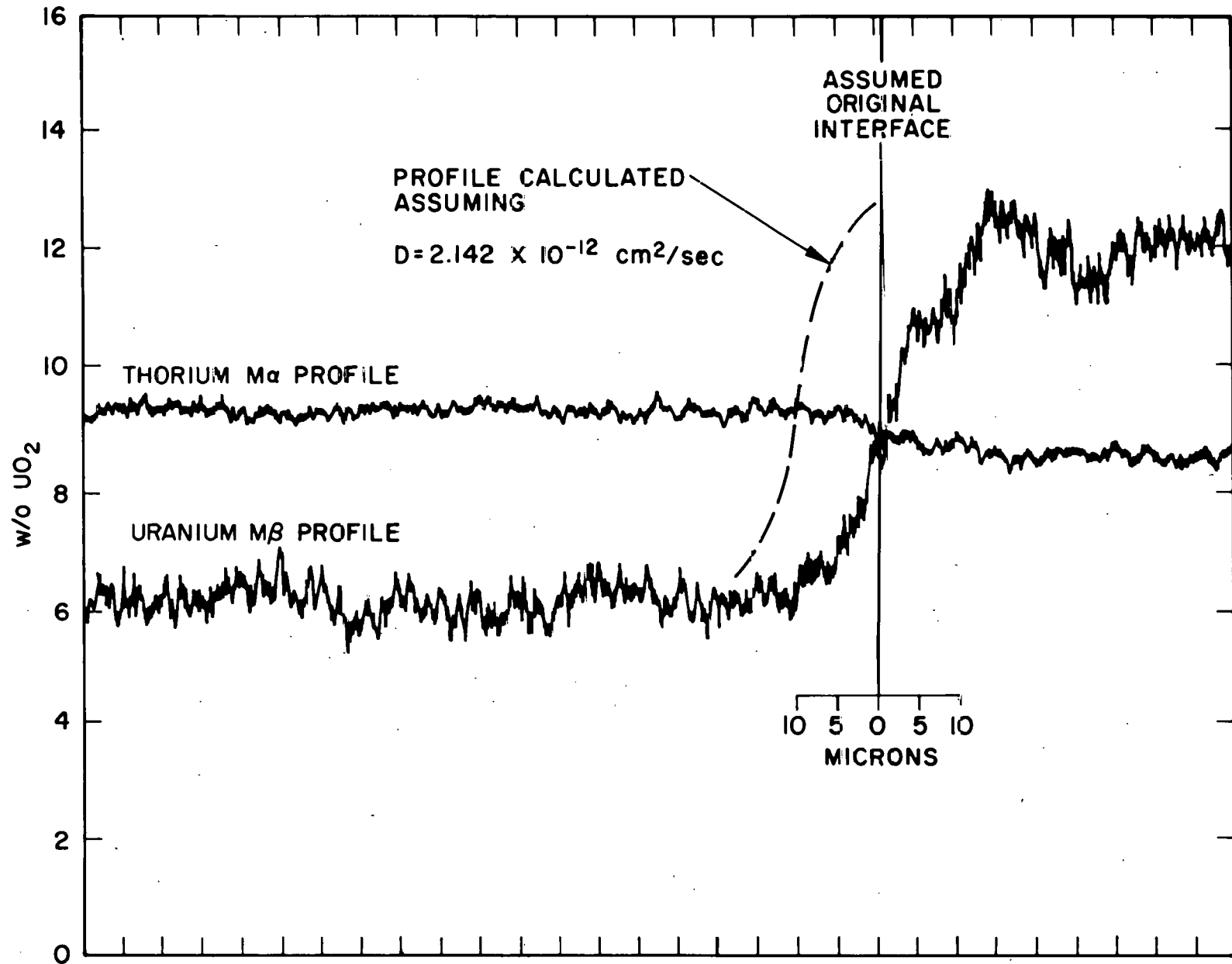


Figure 2. Electron Probe Profiles Across a Typical Interface

of clarity. Both figures include thorium profiles. Since the relative change in thorium content is much less than that for uranium, the inhomogeneities are not shown as clearly on the thorium recorder trace.

IV. AUTORADIOGRAPHY

A. Sample Preparation

Samples for autoradiography are carefully ground as flat as possible, using 45 μ m diamond paste. They are then moved to a glove box illuminated by safe-lights, where they are mounted in spring-loaded fixtures which press the samples upward against the photographic plates. The plates are glass slides, approximately 25 x 76 mm, coated with Kodak NTA emulsion. Typical exposure time for LWBR binary fuels is 30 to 55 minutes. Ten samples are exposed in the same spring-loaded fixture. An opaque cover is placed over the fixture, with the plates and samples, during exposure.

Development is in Kodak D-19 solution, according to the manufacturer's instructions. The mean photographic density of the resulting sample image generally lies between 0.4 and 0.6. Typical inhomogeneities appear as dark spots, with photographic densities above 0.8. Atypical dilute inhomogeneities appear as larger gray patches with a photographic density 0.1 to 0.2 units greater than the mean for the sample.

B. Calibration

Photographic density is defined by the equation

$$D = -\log_{10} (T/T_0) \quad (\text{Eq. 8})$$

where T/T_0 is the fraction of incident light transmitted through the plate. A photographic density of 1 therefore signifies that 10% of the light is being transmitted.

In the region between underexposure and overexposure, photographic density varies approximately linearly with the number of α -particle tracks intercepting the emulsion. Photographic density therefore varies approximately linearly with uranium content and exposure time. However, the α -particles that actually darken the plate are not emitted, for the most part, by the U^{233} , the isotope of interest. They are emitted by the U^{232} contaminant and its decay products; the fuel mixtures initially contain from 5.3 to 9.3 ppm of U^{232} . Therefore, the photographic density is a function of both the amount of contaminant

originally present, and the time since purification. These values are constant for any one sample; the U^{232} and daughter-product concentrations at any one time are constant fractions of the U^{233} content, and therefore photographic density varies as U^{233} content. But this fraction is not constant from sample to sample, and therefore the slope of the calibration curve, U^{233} as a function of photographic density, also varies. There must be an internal calibration for each sample.

The calibration is performed in a way essentially analogous to that for the electron probe. A background density is found, and applied to 0 wt% UO_2 ; a mean density is found and set equal to the mean composition; and a straight line is erected between these two points and extended to other compositions by means of Equation 7.

However, the background density B cannot be found by running a blank sample because, at low film densities, the photographic plates are in the region of underexposure, which is non-linear. What is needed is an artificial background B which is calculated by extrapolating the linear portion of the calibration curve downward to zero exposure.

Several different exposures were required in the linear portion of the calibration curve. However, it was not practical to use several samples with differing U^{233} content; such samples would not fall on the same calibration curve, due to different U^{232} content and differing amounts of aging. Instead, a calibration curve was constructed using a single sample, and differing exposure times. The straight portion of this curve was extrapolated to zero time, using least-squares techniques, and the value obtained for B is 0.1024 photographic density units. This value should be applicable to all exposures using Kodak NTA plates and developed in a way comparable to the calibration runs, i.e., strictly according to the manufacturer's recommendations. It should not be necessary, therefore, to redetermine the value of B unless the characteristics of NTA emulsion are changed. The standard deviation associated with the determination of B is 0.0264 density units.

C. Correction for α -particle Range

A point source of α -particles on a photographic plate will produce a dark circle with a diameter equal to twice the range of the α -particles in the

photographic emulsion. Steigert et al. (Reference 6) give values for this range in Kodak NTA emulsion for several different α -particle energies. In the range below 8 Mev, their data may be fitted to the equation

$$R = \frac{E}{0.337 - 0.01683 E} \quad (\text{Eq. 9})$$

where

R = range in μm

E = α -particle range in Mev.

U^{233} emits α -particles at energies of 4.77 and 4.82 Mev. Substitution of these values for E in Equation 9 gives values of 18.58 and $18.83\mu\text{m}$, respectively. The circular area produced by a point source would therefore be approximately $37\mu\text{m}$ in diameter. All diametral measurements of high-urania features on the autoradiographic plate are therefore too large by this amount; an $18\mu\text{m}$ halo surrounds the image of the urania-rich area, and cannot be distinguished from it.

In order to verify Steigert's results by direct observation, an autoradiograph was made of a thin sliver of fuel. The width of the sliver was measured at 16 locations on carefully scaled photomicrographs of the fuel, and at the corresponding 16 locations on the autoradiograph. The width of the autoradiograph image was greater in every case; the mean of the differences was $29\mu\text{m}$, with a standard deviation of $10\mu\text{m}$. This is within one standard deviation of the values predicted from Steigert's measurements, and apparently establishes that the expected enlargement of images does indeed take place to approximately the extent predicted.

In the evaluation of autoradiographs, the range of $29\mu\text{m}$, from the above determination, is used as the diameter correction, rather than the value of $37\mu\text{m}$ indicated by the Steigert data. In the routine evaluation of an autoradiograph, the inhomogeneities are counted by 1-mil ($25.4\mu\text{m}$) size classes (1-2, 2-3 mils, etc.). The mid-point of each of these size classes (1.5, 2.5, 3.5 mils) is then found, and 1.14 mils ($29\mu\text{m}$) is subtracted from these mid-point values to give 0.36, 1.36, 2.36, ... mils (8.6, 34, 59.4, ... μm) as the corrected mean diameter. The total area of the inhomogeneities in each size class is then calculated as if all inhomogeneities had diameters equal to the corrected mean diameter of their size class. The total corrected area of inhomogeneity appearing in the surface may then be found by summing all the size classes, and it is expressed as a percentage of the total autoradiographed surface

of fuel. The assumption is then made that this percentage represents the volume percentage of segregations, each of which consists entirely of 100% dense, pure urania. The fuel was acceptably homogeneous for LWBR purposes if this percentage was less than the value given in Table I for the particular type of fuel examined.

D. Use of the Microdensitometer

If large ($>254\mu\text{m}$), dilute inhomogeneities are observed, or if unusual conditions are observed during routine evaluation, the autoradiograph is quantitatively evaluated by the Joyce-Loebl Microdensitometer. The photographic density of the autoradiographic plate is measured through an aperture $127 \times 127\mu\text{m}$ in size, and recorded continuously along several millimeters of random straight traverse. Alternatively, a traverse may be made through the diameter of a large feature, which is marked in advance. As with the electron probe, the horizontal distance along the recorder chart represents the position on the traverse, and the vertical position of the pen trace varies approximately linearly with mole % urania, at least in the central part of its range. As previously discussed, the calibration of the microdensitometer in terms of urania content is essentially analogous to the procedure with the electron probe; Equation 7 applies, with $B = 0.1024$.

However, there are some important differences between an electron probe, set up to monitor the uranium $M\beta$ peak, and the combination of the microdensitometer and the photographic plate. This can be seen by comparing typical microdensitometer results (Figure 3) with electron probe results (Figures 1 and 2). The microdensitometer is degraded by more than an order of magnitude, both in sensitivity and in resolution. The sharp focus of the electron probe is a circle $3\mu\text{m}$ in diameter; the smallest practical aperture of the microdensitometer is a square $127\mu\text{m}$ on each side, with 2300 times the area of the electron beam focus. The response of the emulsion, in photographic density, is approximately linear with uranium content only in the region between underexposure and overexposure, and is far less linear and reproducible even in this region than the electron probe response.

Furthermore, the inhomogeneity peaks appearing on the microdensitometer scans must be corrected for the effect of α -particle range. Since a random traverse crosses the α -particle halo at an oblique angle, this correction is, in the general case, somewhat greater than twice the range of $14.5\mu\text{m}$. As a

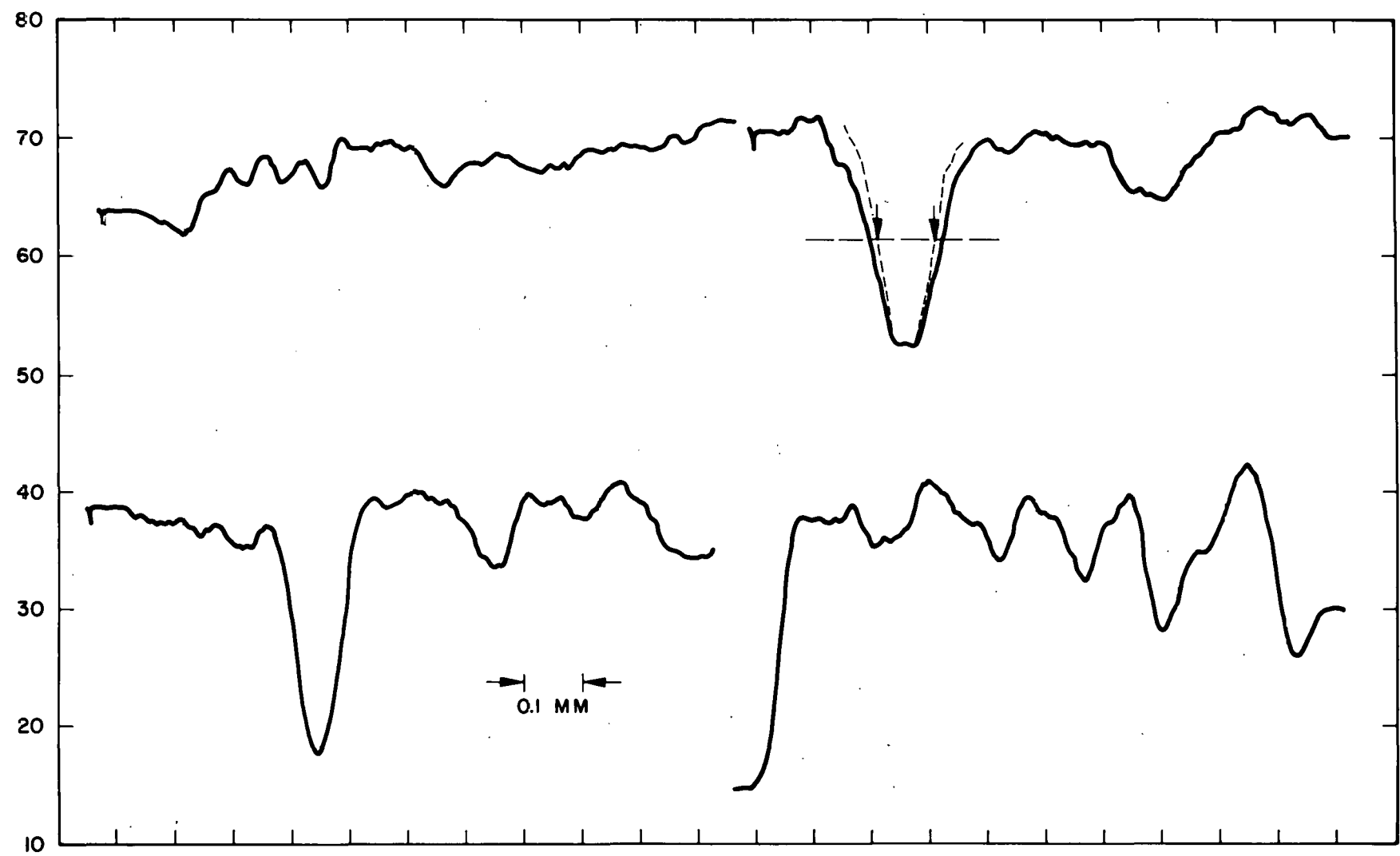


Figure 3. Typical Microdensitometer Traverses, Showing Method of Profile Correction

result of calculations presented in Appendix I, a correction of $38\mu\text{m}$ was used. Such a correction is shown on one of the peaks of Figure 3. A second peak is constructed graphically, with an amplitude comparable to the observed peak, but with a peak breadth that is $38\mu\text{m}$ less along a line at half the maximum amplitude.

E. Interpretation of Microdensitometer Profiles

The resulting profile may be interpreted in essentially the same was as the recorder charts produced by the electron probe. The chart value corresponding to 3 wt% UO_2 over nominal composition is determined using Equation 7, with $B = 0.1024$ density units. The chart area of inhomogeneity peaks that have photographic densities exceeding this value continuously for $10\mu\text{m}$ is determined. It is then obtained as a percentage of the total chart area representing photographic densities greater than background. This percentage may then be compared to Table I.

The microdensitometer was used only for inhomogeneities with mean diameters greater than $400\mu\text{m}$. An attempt was made to extend its usefulness to smaller sizes. The resolution of the instrument is fixed by the diagonal of the minimum aperture, which is $180\mu\text{m}$. As the diameters of inhomogeneities are decreased below this value, the apparent width of the peak on the recorder chart remains the same, but the amplitude of the peak decreases as the square of the diameter of the inhomogeneity. Since this procedure is of interest only for inhomogeneities that have already produced images of low photographic density, the resulting peaks quickly become lost in the random noise of the results. Where the autoradiograph indicates that a sizeable portion of the sample's uranium may be contained in inhomogeneities less than $250\mu\text{m}$ in diameter, and with a composition substantially less than 100 wt% urania, then the original sample itself is reevaluated by the electron probe.

F. Criteria for Rejecting Artifacts

In microdensitometer work, as well as in autoradiographs evaluated by counting, it is necessary to reject artifacts. These are dark regions on the emulsions caused by dust, abrasion, emulsion imperfections, and other causes that cannot be completely eliminated, regardless of the care used in storing, exposing, and developing the plates. Generally, inspectors reject artifacts on the basis of their atypical appearance when examined at 10x magnification.

Among the features that may serve to distinguish artifacts are the following:

1. The absence of a diffusion zone
2. Details smaller in dimension than twice the alpha-particle range (29 microns)
3. Radii sharper than the alpha-particle range (14.5 microns).

It is also of critical importance that the autoradiograph be sharp. Figures 4 and 5 are 10x enlargements of two autoradiographs, made by placing the original autoradiographs in the negative carrier of a photographic enlarger. They are therefore negative images; the white regions shown in the figures actually are fuel overloads which are black on the original autoradiographs.

Figure 4 was made by a flat sample, in excellent contact with the plate. It includes many spots close to the minimum diameter of twice the alpha particle range. In Figure 5, the contact was not satisfactory. As a result, the spots are less sharp, and less intense. Since, however, the total area of spots is determined in the routine size-class count, the sample of Figure 5 appeared to have a much greater area of inhomogeneity, and therefore to be much less homogeneous than that of Figure 4. Actually, the two samples came from the same batch, and detailed studies using the microdensitometer showed that they had a comparable degree of homogeneity.

It is therefore necessary to eliminate inferior autoradiographs such as Figure 5 from consideration. Any autoradiograph that has no counts, or very few, recorded in the 1 to 2 mil size range should be regarded as suspect. An autoradiograph that has all of its small autoradiographic indications on one side may have been in contact only along that side; there may have been a wedge-shaped space between the plate and the sample. However, it is conceivable that material may be produced with no small inhomogeneities, or all of them segregated at one edge of the sample.

In doubtful cases, plates should be studied by microdensitometry. In particular, traverses should be run across the edges of the image, particularly those edges that are suspected of not having been in good contact with the sample. Figure 6 shows two such traverses; one (Sample A) was taken across the edge of Figure 4, and the other (Sample R) was taken across the edge of Figure 5. The slopes of the second scan are considerably less than the first. For a sample properly in contact, such as Sample A, the transition from the

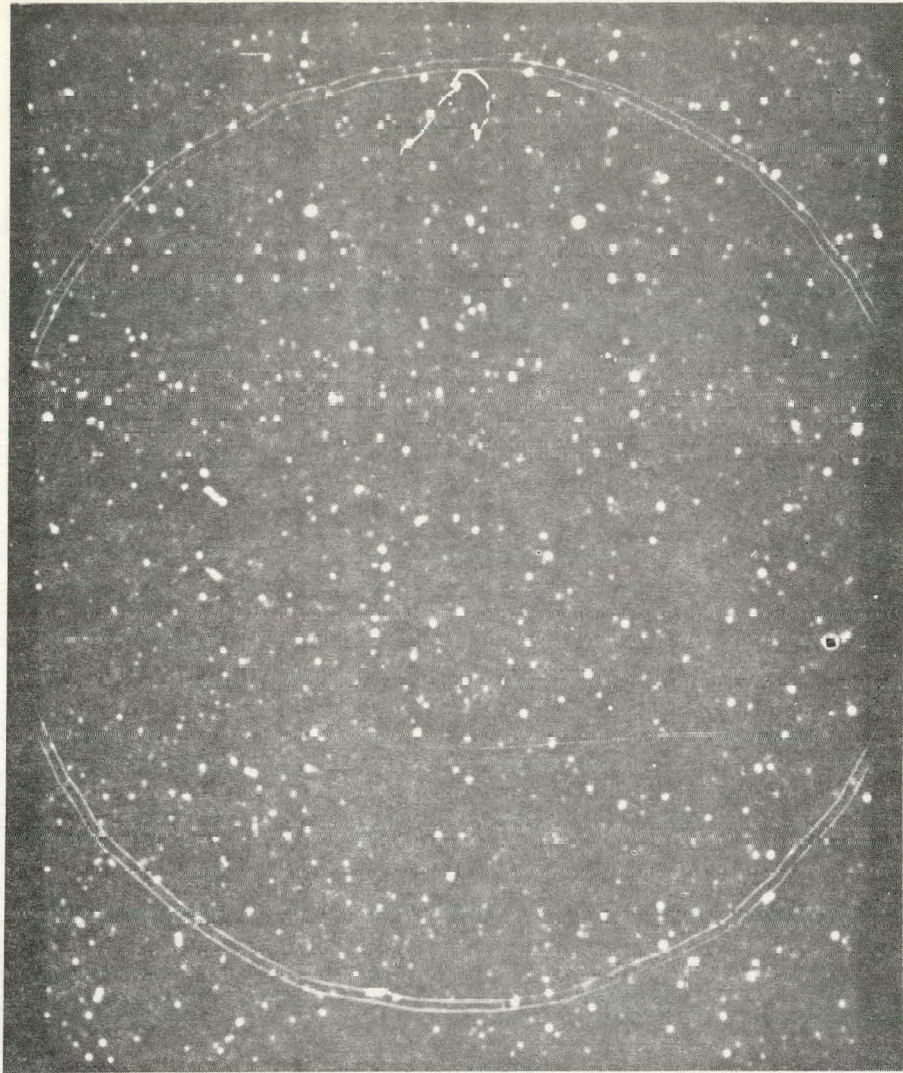


Figure 4. Autoradiograph of Sample A (10x)

typical photographic density of the image, to that of clear glass, is made over a distance comparable to the alpha particle range plus the aperture width. A wider region of transition, such as that for Sample R, is indicative of poor contact.

Optimum photographic density for Kodak NTA plates is 0.5. This is produced by 2.5×10^6 alpha particles/cm² in this particular emulsion. If the surface area of a sample, as exposed in the metallographic mount, is known, and the alpha count rate is determined by means of an appropriate meter, then the appropriate time for optimum exposure can be calculated.

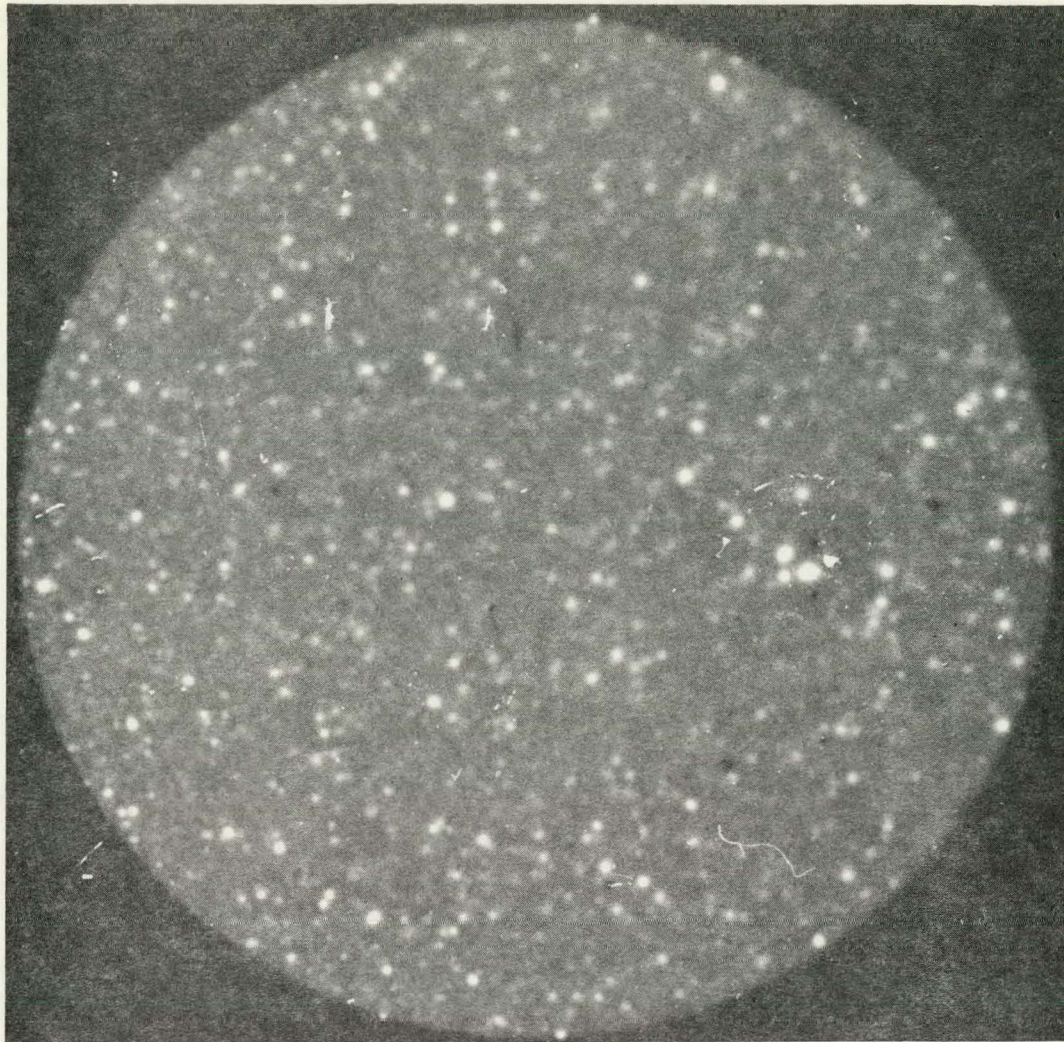


Figure 5. Autoradiograph of Sample R (10x)

V. SUMMARY AND CONCLUSION

In binary fuels, segregations abnormally high in uranium, when placed in-pile, can be the sites of elevated temperatures, increased gas accumulation and release, and high and non-uniform swelling. To minimize these segregations, manufacturing procedures have been devised to produce fuels with compositional distributions as uniform as possible. This report discusses the inspection of the resulting fuel pellets, to ensure that the various procedures are of continuing effectiveness in providing homogeneous material.

The principal method of inspecting pellets for homogeneity consists of making autoradiographs of polished surfaces on Kodak NTA plates. After development, the high-urania segregations appear as dark spots. The spots in various

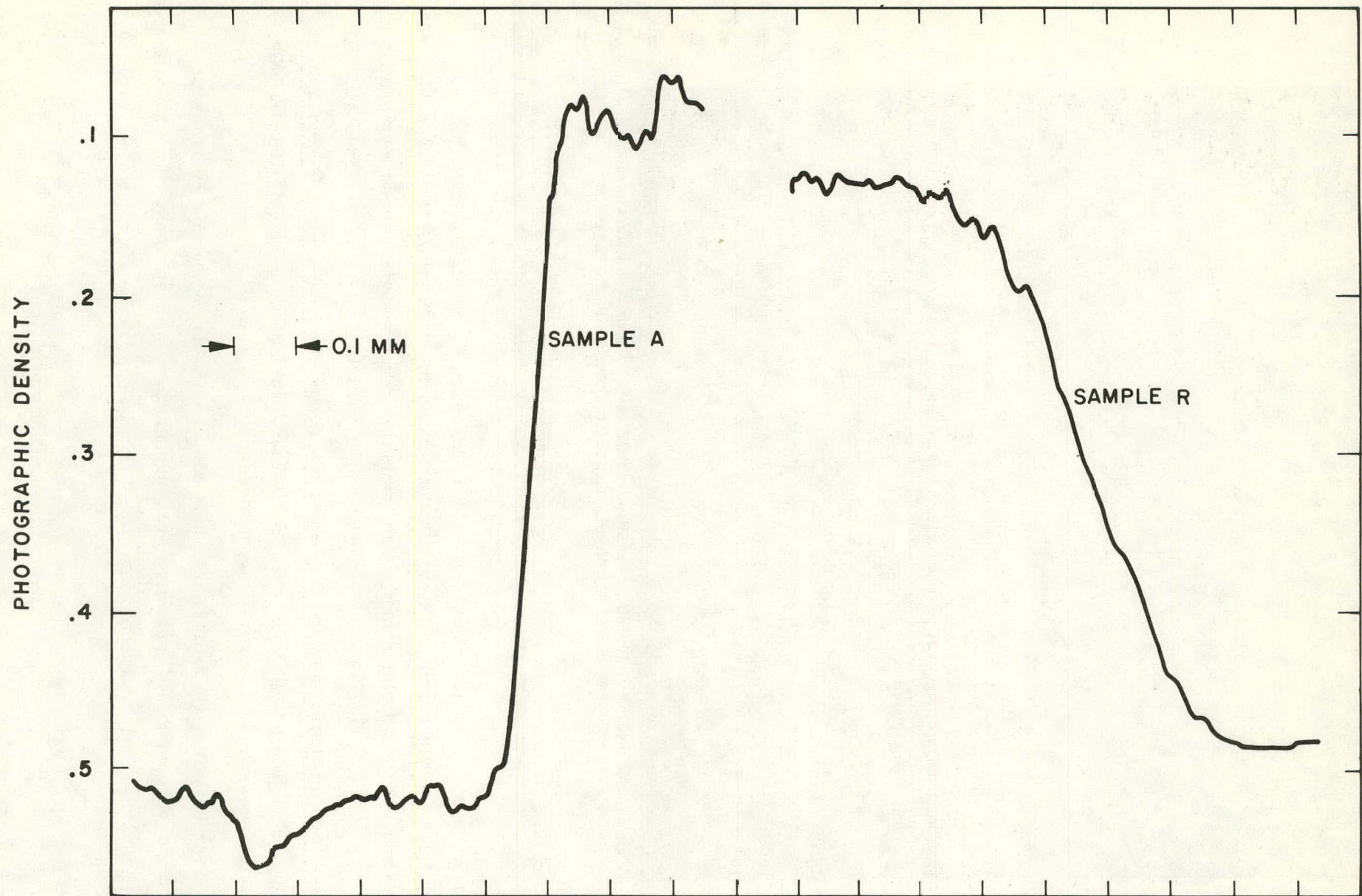


Figure 6. Microdensitometer Traverses Across the Edges of Sample A
(Good Contact) and Sample R (Poor Contact)

size ranges are counted by an inspector. The size ranges are corrected for the effect of alpha-particle range in the emulsion, which increases the apparent diameter of each spot by 29 microns. Finally the total fractional area occupied by the inhomogeneities is calculated.

The method requires a judgment on the part of the inspector as to the size of the inhomogeneity, i.e., where the margin will be placed. There is also no provision for inhomogeneities that have average compositions less than 100 w/o UO_2 ; it is assumed that all normal-appearing inhomogeneities are pure UO_2 . When large, dilute inhomogeneities are observed, the microdensitometer is used for further evaluation.

The judgment of the inspector is also relied upon to reject artifacts and inferior images due to poor contact. However, the high contrast and resolution of the Kodak NTA plates aid in this task. It is possible, by this routine examination of NTA plates, to verify that the current manufacturing process for binary fuels results in a product well within specifications with regard to homogeneity.

When difficulties or marginal cases arise, it is possible to examine the autoradiographic plates quantitatively by means of a microdensitometer. The smallest available aperture is used, and random straight traverses are made across the autoradiograph. This results in a recorder-chart profile of the variation of photographic density with distance along the traverse. In the region between underexposure and overexposure, photographic density varies linearly with uranium content. By setting the extrapolated background equal to zero urania content, and the average photographic density equal to the mean urania content, it is possible to calibrate the plate. The recorder chart trace makes it possible to take into account the variation in composition and density among inhomogeneities. It is therefore possible to calculate, for a large, dilute inhomogeneity, the size of an equivalent inhomogeneity consisting of fully dense, pure urania. This smaller equivalent homogeneity may then be used in the evaluation of the sample.

Finally, the electron probe is available as a reference and research method. The equipment is much more expensive, the sample preparation is more difficult, and a greater degree of skill and amount of time is needed. But resolution, linearity and sensitivity are better by an order of magnitude or more, and the examination can be extended to elements other than uranium if questions arise as to their presence or effect.

ACKNOWLEDGMENTS

The author is indebted to T. J. Burke and R. W. Reidl for the manufacture of samples; to O. O. M. Gamba and T. Anater for electron probe work; and to J. Belle for review of the manuscript.

REFERENCES

1. R. M. Berman, "The Homogenization of ThO_2 - UO_2 (LWBR Development Program)," WAPD-TM-1051 (December 1972).
2. F. N. Rhines and R. A. Colton, "Homogenization of Copper-Nickel Powder Alloy," Trans. Am. Soc. Metals, Vol. 30, pp. 168-188 (1942).
3. A. D. King, "Thorium Diffusion in Single-Crystal Thoria," J. Nucl. Mat., Vol. 38, pp. 347-349 (1971).
4. D. K. Riemann and T. C. Lundy, "Diffusion of ^{233}U in UO_2 ," J. Am. Ceram. Soc., Vol. 52, pp. 511-512 (1969).
5. R. E. Ogilvie, "Quantitative Electron Microprobe Analysis, in X-ray and Electron Methods of Analysis," H. Van Olphen, ed., pp. 55-75, Plenum Publishing Co., New York, 1968.
6. F. E. Steigert, E. C. Toops, and M. B. Sampson, "Alpha-Particle Range-Energy Curve for Kodak NTA Emulsions," Physical Review, Vol. 83, p. 474 (1951).

APPENDIX I

AVERAGE TRAVERSE INCREMENT CAUSED BY INCREASE IN APPARENT
DIAMETER OF INHOMOGENEITIES BY ALPHA-PARTICLE RANGE

APPENDIX I

AVERAGE TRAVERSE INCREMENT CAUSED BY INCREASE IN APPARENT DIAMETER OF INHOMOGENEITIES BY ALPHA-PARTICLE RANGE

In Figure A-1, the high-urania region in contact with the autoradiographic plate is a circle with radius, r . However, the range of alpha particles in the photographic emulsion is a , and the radius of the dark circle on the autoradiograph is therefore $r + a$.

A random microdensitometer traverse PQMN shows a continuous dark area in the segment PN. If the range a had been zero, it would be possible to detect segments such as MQ, and calculate the fraction of such segments in the total random traverses. This fraction would constitute the proportion of high-urania material in the surface, and, since this surface is assumed typical, in the entire sample volume.

It is therefore desired to subtract segments PQ and MN from each observed dark segment, PN, in order to permit the remainders of these segments, MQ, to be added together. It appears, from Figure A-1, that $PQ + MN$ will be somewhat greater than $2a$ in the general case. PN is a chord of the larger circle with a radius $r + a$, and QM is a chord of the smaller circle with a radius r ; the required correction is the difference between these two chords. The formula for the lengths of chords is given in Equation A-1 for chord \overline{MQ}

$$\overline{MQ} = 2r \sin \theta \quad (\text{Eq. A-1})$$

$$\cos \theta = \frac{r - h}{r} \quad (\text{Eq. A-2})$$

or, alternatively, we can state simply that the chord length is a function of r and h ;

$$\overline{MQ} = f(r, h) \quad (\text{Eq. A-3})$$

$$\overline{NP} = f(r+a, h+a) \quad (\text{Eq. A-4})$$

$$\text{Transverse correction } T = \overline{NP} - \overline{MQ} \quad (\text{Eq. A-5})$$

It is not necessary to integrate the actual function for T , since the result must be the area of the annulus:

$$\int_0^{2r+2a} T = \pi(r + a)^2 - \pi r^2 \quad (\text{Eq. A-7})$$

$$= a\pi(2r + a)$$

RANDOM
MICRODENSITOMETER
TRAVERSE

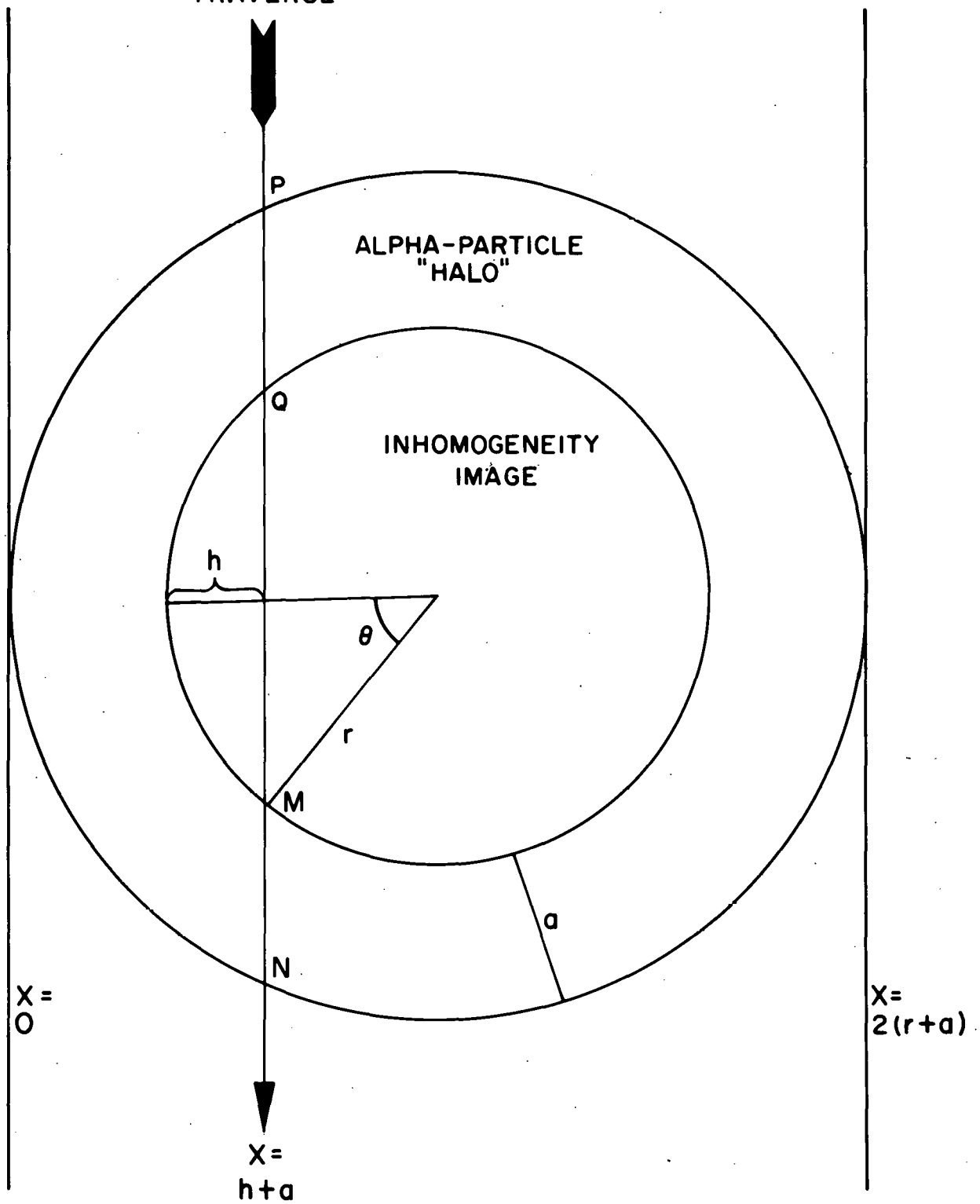


Figure A-1. Random Microdensitometer Traverse
Across Inhomogeneity Image

$$T_M = \frac{a\pi(2r + a)}{2(r + a)} \quad (\text{Eq. A-8})$$

For a point source of urania, r is negligible with respect to a , and the average correction is 1.5708 a . For large segregations, a is small with respect to r , and the average correction approaches a . For $a = 14.5$ microns, the following values of T_M can be calculated for various values of r between 10 and 50 microns.

TABLE A-I. MEAN CHORD INCREMENT, MICRONS, DUE TO
ALPHA-PARTICLE RANGE IN EMULSION

<u>True Radius</u>	Range = 14.5 Microns		<u>Increase In Mean Chord, Microns</u>
	<u>Apparent Radius</u>	<u>Apparent Diam., Mils</u>	
10	24.5	1.92913	32.0731
20	34.5	2.71654	35.9803
30	44.5	3.50394	38.1315
40	54.5	4.29134	39.4933
50	64.5	5.07874	40.4328

An approximate weighted average for the correction, for a typical inhomogeneity in LWBR binary fuel, is 38 microns or 1.5 mils. This quantity should be subtracted from the size of each inhomogeneity observed on the micro-densitometer traverses, before their length as a fraction of the total is calculated. Inhomogeneities with an apparent size less than 38 microns, measured along the traverse, should be ignored.

APPENDIX II

LWBR CORE REFERENCE PROCEDURES

APPENDIX II

LWBR CORE REFERENCE PROCEDURES

The general procedure and minimum requirements necessary to produce and evaluate an autoradiograph of an LWBR ceramic type uranium enriched pellet for the purpose of determining the volume percent of inhomogeneous particles within the pellet are discussed in this section.

Longitudinal and transverse pellet surfaces prepared for metallographic attribute evaluation are ground as flat as possible, using 45-micron diamond compound for the final surface treatment. This is followed by ultrasonic cleaning and oven drying.

Samples are then mounted, together with '3" x 1" Kodak NTA plates, in special spring-loaded jigs which exert upward pressure on the backs of the metallographic mounts, holding them against the emulsion of the plate. This is done in a glove-box, by safelight illumination. Precautions must be taken to avoid abrasion of the emulsion surface.

After the jig is loaded, a light-tight, bell-shaped metal cover is placed over it during the exposure. The length of exposure may be determined by experience. Alternatively, the activity at the sample surface may be measured, by placing an alpha survey meter probe (PAC-4 or comparable) close to the surface and noting the dial reading, and the area of the sample exposed on the surface is determined. The optimum exposure, which should result in a photographic density of 0.5 on NTA plates, is the time necessary to accumulate 2.5×10^6 counts per cm^2 of exposed surface.

The development, fixing, washing, and drying of the plates follow the manufacturer's recommendations. The photographic solutions become contaminated and handling and disposal follow appropriate Radcon procedures. In order to minimize the amount of contaminated liquid waste, the volume of working solutions is adjusted for maximum utilization in processing.

After the autoradiograph is dry, the emulsion surface, which may be contaminated, must be sealed. A clean glass slide of high optical quality is placed on this surface, and the edges of the plate and the slide are taped in such a way as to close off the emulsion surface from the environment. The tape must have permanent warning markings against removal. After appropriate cleaning and monitoring, the autoradiograph may then be examined in a clean area.

The average photographic density of the image may be obtained by using a Kodak shop densitometer; acceptable autoradiographs have average photographic densities between 0.35 and 0.65. The general quality of the image is then evaluated for sharpness and artifacts by comparison with established standards representative of the process. Artifacts may be distinguished by the following criteria; however, this list should not be considered exhaustive:

- (1) Parallel dark scratches, indicating abrasion
- (2) Pinholes in the emulsion
- (3) Plate defects or foreign particles adhering to the plate (These can be mistaken for inhomogeneous areas.)
- (4) Absence of a diffusion zone
- (5) Diameters less than 15 microns
- (6) Radii of curvature less than 15 microns at any periphery of the feature.

The inspector also reviews the plate for fogging, blemishes, water marks, and stains which may interfere with interpretation of the autoradiographic image. After the inspector is satisfied that the image is of acceptable quality, the inhomogeneities are counted by one-mil size classes (1-2 mils, 2-3 mils, etc.). There should be no inhomogeneities in the 0-1 mil size class. The inhomogeneous area, measured at a magnification of 56x, appears as a dark indication against the lighter matrix background. The size class is determined by the mean diameter of the dark area measured between points at which there is an observed contrast against the image background. An inhomogeneity is here defined as UO_2 particles that are not completely reacted with the matrix resulting in areas that have a higher uranium enrichment than the matrix.

The total area of inhomogeneities expressed as a function of the area of the autoradiographic image is determined. The area fraction A of inhomogeneities in the size class i , with midpoint mean diameter \bar{d}_i corrected for alpha particle range, and frequency per class N_i is:

$$A = \sum_{i=1}^n \frac{N_i \bar{d}_i^2}{D}$$

where D = average diameter of evaluated autoradiographic image.

Determination of the volume percent v/o of inhomogeneous particles in a pellet is based on the assumption that the volume fraction is equal to the area fraction of the autoradiographic image for the case of spherical particles of random size and random distribution. If the total v/o of inhomogeneities falls below the limits set in Table I, the material may be judged at this stage to have passed the homogeneity specification. If the total v/o of inhomogeneities exceeds the limits of Table I and contains indications ≥ 10 mils or there are inhomogeneities with mean diameters ≥ 15 mils, the autoradiograph is examined by microdensitometry.

An effective aperture of 5 mils square is used, and the linear translation magnification lever system is set at 10x. Cross sections are run for each indication ≥ 10 mils mean diameter, and calibration standards are scanned on the same recorder graph. Also, a random traverse is made to determine the average recorder chart reading, R_A , for Equation 7.

The calculated volume percent (v/o) of inhomogeneities smaller than 10 mils in mean diameter will be assumed to contain 100% UO_2 . For inhomogeneities ≥ 10 mils the calculated volume percent will be corrected to an equivalent volume percent of 100% UO_2 inhomogeneous particles utilizing the urania concentration determined by microdensitometry and appropriate correction curves developed for each pellet type.

If there are inhomogeneities with mean diameters ≥ 15 mils, the maximum acceptable inhomogeneity size will be established utilizing urania concentration determined by microdensitometry and appropriate "clump" size/"clump" enrichment correction curves developed for each LWBR pellet type.

In certain special cases, in which the autoradiograph indicates large numbers of small (<10 mil diameter) inhomogeneities with photographic densities less than that for pure UO_2 , it may be desirable to evaluate the material by means of electron probe, if the calculated v/o inhomogeneity does not meet the specification requirement. Random traverses are run of the uranium M emission line. Next, the total area is determined of all peaks exceeding the average intensity by 3 w/o for more than 10 microns along the traverse. The resulting value is compared to the total area between background and the recorder trace to determine if the percentage of the total area of the inhomogeneities is less than 10% of the total area between the background and the recorder trace. If this condition is met, the material will be considered as meeting homogeneity specification. The criterion of 10% of the sample's uranium in the inhomogeneities was the initial assumption used in establishing the specification.